

# Probability for cluster formation in the trans-tin and trans-lead nuclei

R K Biju, Sabina Sahadevan and \*K P Santhosh

School of Pure and Applied Physics, Kannur University, Payyanur Campus, Payyanur 670 327, India

\* email: drkpsanthosh@gmail.com

## Introduction

Clustering is a very general phenomenon, which appears in atomic, nuclear, sub nuclear, and the cosmic worlds [1]. A direct indication of clustering is the emission of alpha particle or heavier clusters from heavy nuclei. Clustering properties of nuclei would be helpful to obtain a systematic understanding of both the stable and exotic nuclei. The present work aims to study the possibility of clustering in heavy nuclei by computing the cluster formation probability for the entire experimentally observed cluster decays from carbon to silicon taking the Coulomb and proximity potential as interacting barrier for the post-session region and simple power law interpolation for overlap region. We have also computed the cluster formation probability for different C, O, Ne and Mg clusters from  $^{112,114}\text{Ba}$ ,  $^{116,118}\text{Ce}$ ,  $^{120,122}\text{Nd}$  and  $^{124,126}\text{Sm}$  parents in the trans-tin region.

## The model

The interacting potential barrier [2] for a parent nuclei exhibiting exotic decay is given by  $V = Z_1 Z_2 e^2 / r + V_p(z)$  for  $Z > 0$  (1)

Here  $Z_1$  and  $Z_2$  are the atomic numbers of daughter and emitted cluster  $z$  is the distance between the near surfaces of the fragments and  $V_p$  is the proximity potential. The barrier penetrability  $P$  is given as

$$P = \exp\left\{-\frac{2}{\hbar} \int_a^b \sqrt{2\mu(V-Q)} dz\right\} \quad (2)$$

The half life time is  $T_{1/2} = \ln 2 / nP$ , where  $n$  is the assault frequency. The cluster formation probability,  $S$  can be calculated within the fission model as the penetrability of the internal part (overlap region) of the barrier is  $S = \exp(-K)$

Here, 
$$K = \frac{2}{\hbar} \int_a^0 \sqrt{2\mu(V-Q)} dz \quad (3)$$

$a$  is the inner turning point and is defined as  $V(a) = Q$  and  $z = 0$ , the touching configuration.

## Results discussion and conclusion

Fig.1 represents the plot for computed  $\log_{10}(S)$  versus  $A_2$ , mass number of the fragment, for the emission of different C clusters from  $^{112,114}\text{Ba}$ , O clusters from  $^{116,118}\text{Ce}$ , Ne clusters from  $^{120,122}\text{Nd}$  and Mg clusters from  $^{124,126}\text{Sm}$  parents respectively. The  $Q$  values are computed using the experimental binding energies of Audi et al [3] and some masses are taken from the table of KTUY [4]. It is clear from the plot that the maximum value for preformation probability is obtained for  $^{12}\text{C}$ ,  $^{16}\text{O}$ ,  $^{20}\text{Ne}$  and  $^{24}\text{Mg}$  clusters from the corresponding parents. As considered the neutron proton asymmetry distribution in light clusters by the  $N/Z$  ratio of the matter at the centre of the nuclei, for  $N = Z$  matter means that the neutron and proton distribution is symmetrical and only the alpha particle like matter exist at the centre of the nuclei. Therefore we would like to point out that the clusters  $^{12}\text{C}$ ,  $^{16}\text{O}$ ,  $^{20}\text{Ne}$  and  $^{24}\text{Mg}$  form alpha like cluster configurations in the parent nucleus.

Fig. 2 represents the plot for  $\log_{10}(S)$  versus  $A_2$ , mass number of various C clusters from Ra, Fr, Ac and Th parents. It is evident from the plot that a peak in cluster formation probability is obtained at  $^{14}\text{C}$  nucleus. We would like to point out that the  $^{14}\text{C}$  cluster emission from different Ra, Fr, Ac and Th parent nuclei has already been

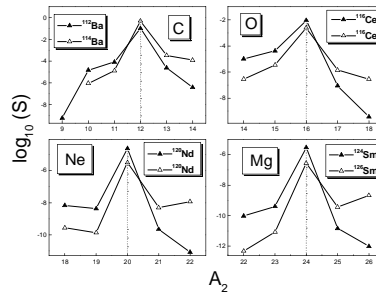


Figure 1: Plot for  $\log_{10}(S)$  versus mass  $A_2$ , of C,O,Ne,Mg clusters from Ba,Ce,Nd,Sm parents.

detected experimentally. So the  $^{14}\text{C}$  cluster preforms in these parents, as compared to other carbon clusters. We have also computed the preformation probability of different O isotopes from  $^{226,228}\text{Th}$  and  $^{21-25}\text{F}$  clusters from  $^{231}\text{Pa}$ . It is found that in the case of  $^{228}\text{Th}$  parent the maximum value of preformation probability is obtained for  $^{20}\text{O}$  and in the case of  $^{231}\text{Pa}$  isotope the maximum value is obtained for  $^{23}\text{F}$  cluster.

Fig. 3 represents the plot for  $\log_{10}(S)$  versus  $A_2$  for the emission of different Ne clusters from various U, Th and Pa parents. It is clear from the plot that two peaks are present at  $A_2 = 24$  and  $26$ . In the case of  $^{232}\text{Th}$  and  $^{234,236}\text{U}$  parents the  $^{24,26}\text{Ne}$  clusters are experimentally detected but  $^{26}\text{Ne}$  has the maximum cluster formation probability compared to  $^{24}\text{Ne}$  cluster. Again the parents  $^{230}\text{Th}$ ,  $^{231}\text{Pa}$ ,  $^{232,233,235}\text{U}$  have the maximum cluster formation probability for  $^{24}\text{Ne}$  cluster as compared to  $^{26}\text{Ne}$  cluster, i.e these clusters are formed very fast in these parents as compared to other clusters.

Fig. 4 represents the plot for  $\log_{10}(S)$  versus  $A_2$  for the emission of  $^{26-32}\text{Mg}$  clusters from various  $^{232-236}\text{U}$ ,  $^{237}\text{Np}$ , and  $^{236,238}\text{Pu}$  parents. It is clear from the plot that the highest peaks are found at  $^{28,30}\text{Mg}$ , the experimentally observed cluster decay. In the case of  $^{232-235}\text{U}$ ,  $^{236}\text{Pu}$  the maximum cluster formation probability is obtained for  $^{28}\text{Mg}$  cluster. For the parents  $^{236}\text{U}$  and  $^{238}\text{Pu}$  the  $^{28,30}\text{Mg}$  clusters are experimentally detected with same half life, but the highest peaks in cluster formation probability is obtained for  $^{30}\text{Mg}$  as compared to  $^{28}\text{Mg}$  cluster. i.e. the  $^{30}\text{Mg}$  cluster has the greater chances for emission from these parents. In  $^{237}\text{Np}$  isotope the  $^{30}\text{Mg}$  cluster has the highest cluster formation probability. We have also found that the  $^{34}\text{Si}$  cluster has the maximum preformation probability from  $^{240}\text{Pu}$ ,  $^{241}\text{Am}$  and  $^{242}\text{Cm}$  parents.

In brief our study reveals that  $^{14}\text{C}$ ,  $^{18,20}\text{O}$ ,  $^{23}\text{F}$ ,  $^{24,26}\text{Ne}$ ,  $^{28,30}\text{Mg}$  and  $^{34}\text{Si}$  clusters have the maximum cluster formation probability in trans-lead region and  $^{12}\text{C}$ ,  $^{16}\text{O}$ ,  $^{20}\text{Ne}$  and  $^{24}\text{Mg}$  clusters have the maximum cluster formation probability in trans-tin region and are due to the double shell closure of  $^{208}\text{Pb}$  and  $^{100}\text{Sn}$  daughter respectively. Alpha like structures are probable for emission (maximum cluster formation probability) from trans-tin region and non-alpha like structures are probable for emission from trans-lead region

which shows the role of neutron proton symmetry and asymmetry of daughter nuclei in these two cases.

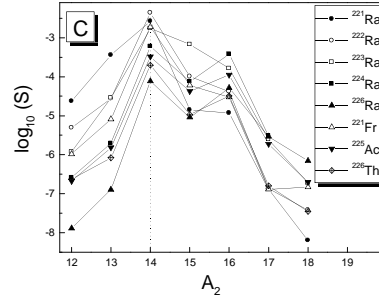


Figure 2: Plot for  $\log_{10}(S)$  versus mass  $A_2$ , of various C clusters from Ra,Fr,Ac and Th parents.

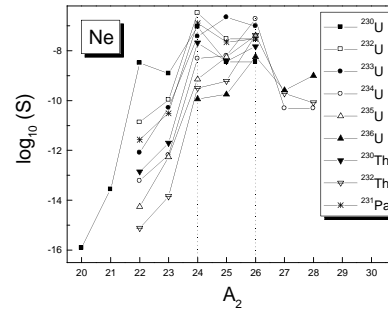


Figure 3: Plot for  $\log_{10}(S)$  versus mass  $A_2$ , of various neon clusters from U, Th and Pa parents.

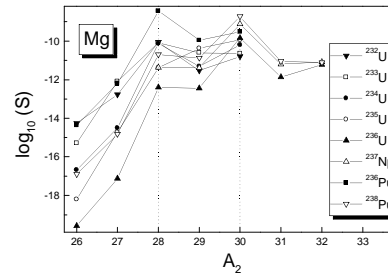


Figure 4: Plot for  $\log_{10}(S)$  versus mass  $A_2$ , of various Mg clusters from U, Np, and Pu parents.

### References

- [1] W Greiner, Z. Phys. A **349** 315 (1994)
- [2] K P Santhosh, R K Biju and A Joseph, J. Phys. G: Nucl. Part. Phys. **35** 085102 (2008)
- [3] G Audi et al, Nucl. Phys. A **729** 337 (2003)
- [4] H Koura et al, Prog. Theor. Phys. **113** 305 (2005)